Lidar equation for ocean surface and subsurface

Damien Josset, Peng-Wang Zhai, Yongxiang Hu, Jacques Pelon, Patricia L. Lucker

Lidar equation for ocean surface and subsurface

Damien Josset,[1,2,*] Peng-Wang Zhai,[2] Yongxiang Hu,[3] Jacques Pelon,[4] Patricia L. Lucker[5]

[1]NASA Postdoctoral Program Fellow, NASA Langley Research Center, Hampton, VA, USA
[2]SSAI 1 Enterprise Parkway Suite 200, Hampton, Virginia, 23666 USA
[3]MS 475 NASA Langley Research Center, Hampton, VA 23681-2199 USA
[4]LATMOS, UMR 8190 CNRS / Université Pierre et Marie Curie, France
[5] SSAI MS 475 NASA Langley Research Center, Hampton, VA 23681 USA
**damien.josset@aero.jussieu.fr*

Abstract: The lidar equation for ocean at optical wavelengths including subsurface signals is revisited using the recent work of the radiative transfer and ocean color community for passive measurements. The previous form of the specular and subsurface echo term are corrected from their heritage, which originated from passive remote sensing of whitecaps, and is improved for more accurate use in future lidar research. A corrected expression for specular and subsurface lidar return is presented. The previous formalism does not correctly address angular dependency of specular lidar return and overestimates the subsurface term by a factor ranging from 89% to 194% for a nadir pointing lidar. Suggestions for future improvements to the lidar equation are also presented.

OCIS codes: (010.0010) Atmospheric and oceanic optics; (280.0280) Remote sensing and sensors; (280.3640) Lidar, (010.4450) Oceanic optics.

References and links

1. Y. Hu, K. Stamnes, M. Vaughan, J. Pelon, C. Weimer, D. Wu, M. Cisewski, W. Sun, P. Yang, B. Lin, A. Omar, D. Flittner, C. Hostetler, C. Trepte, D. Winker, G. Gibson, and M. Santa-Maria, "Sea surface wind speed estimation from space-based lidar measurements," Atmos. Chem. Phys. Discuss. **8**(1), 2771–2793 (2008).
2. D. Josset, J. Pelon, and Y. Hu, "Multi-Instrument Calibration Method Based on a Multiwavelength Ocean Surface Model," IEEE Geosci. Remote Sens. Lett. **7**(1), 195–199 (2010), doi:10.1109/LGRS.2009.2030906.
3. S. Tanelli, S. L. Durden, E. Im, K. S. Pak, D. G. Reinke, P. Partain, J. M. Haynes, and R. T. Marchand, "Cloudsat's Cloud Profiling Radar after two years in Orbit: Performance, Calibration and Processing," IEEE Trans. Geosci. Rem. Sens. **46**(11), 3560–3573 (2008).
4. J. L. Bufton, F. E. Hoge, and R. N. Swift, "Airborne measurements of laser backscatter from the ocean surface," Appl. Opt. **22**(17), 2603–2618 (1983).
5. R. T. Menzies, D. M. Tratt, and W. H. Hunt, "Lidar in-space technology experiment measurements of sea surface directional reflectance and the link to surface wind speed," Appl. Opt. **37**(24), 5550–5559 (1998).
6. D. M. Winker, J. Pelon, and M. P. McCormick, "The CALIPSO mission: Spaceborne lidar for observation of aerosols and clouds," Proc. SPIE **4893**, 1–11 (2003).
7. C. Flamant, J. Pelon, D. Hauser, C. Quentin, W. M. Drennan, F. Gohin, B. Chapron, and J. Gourrion, "Analysis of surface wind speed and roughness length evolution with fetch using a combination of airborne lidar and radar measurements," J. Geophys. Res. **108**(C3), 8058 (2003).
8. P. Koepke, "Effective reflectance of oceanic whitecaps," Appl. Opt. **23**(11), 1816–1824 (1984).
9. A. Morel, "In-water and remote measurement of ocean color," Boundary-Layer Meteorol. **18**(2), 177–201 (1980).
10. M. J. Kavaya, R. T. Menzies, D. A. Haner, U. P. Oppenheim, and P. H. Flamant, "Target reflectance measurements for calibration of lidar atmospheric backscatter data," Appl. Opt. **22**(17), 2619–2628 (1983).
11. K. N. Liou, An Introduction to atmospheric radiation. Academic Press, 2002.
12. J. Lenoble, M. Herman, J. L. Deuze, B. Lafrance, R. Santer, and D. Tanre, "A successive order of scattering code for solving the vector equation of transfer in the earth's atmosphere with aerosols," J. Quant. Spectrosc. Radiat. Transf. **107**(3), 479–507 (2007).
13. M. I. Mishchenko, J. M. Dlugach, E. G. Yanovitskij, and N. T. Zakharova, "Bidirectional reflectance of flat, optically thick particulate layers: An efficient radiative transfer solution and applications to snow and soil surfaces," J. Quant. Spectrosc. Radiat. Transf. **63**(2-6), 409–432 (1999).
14. J. Pelon, C. Flamant, V. Trouillet, and P. H. Flamant, "`Optical and Microphysical Parameters of Dense Stratocumulus Clouds during Mission 206 of EUCREX'94 as Retrieved from measurements made with the airborne lidar LEANDRE 1," Atmos. Res. **55**(1), 47–64 (2000).

#128261 - $15.00 USD Received 10 May 2010; revised 2 Jul 2010; accepted 20 Jul 2010; published 12 Oct 2010

15. D. E. Barrick, "Rough surface scattering based on the specular point theory," IEEE Trans. Antenn. Propag. **16**(4), 449–454 (1968).
16. C. Cox, and W. Munk, "Measurement of the Roughness of the sea surface from photographs of the sun's glitter," J. Opt. Soc. Am. **44**(11), 838–850 (1954).
17. Z. Li, "C. Lemmerz, U. Paffrath, O. Reitebuch, B. Witschas, "Airborne Doppler lidar investigation of the sea surface reflectance at the ultraviolet wavelength of 355 nm," J. Atmos. Ocean. Technol. (2009), doi:10.1175/2009JTECHA1302.1.
18. F. M. Bréon, and N. Henriot, "Spaceborne observations of ocean glint reflectance and modeling of wave slope distributions," J. Geophys. Res. **111**(C6), C06005 (2006), doi:10.1029/2005JC003343.
19. Y. Liu, X. H. Yan, W. T. Liu, and P. A. Hwang, "The probability density function of ocean surface slopes and its effect on radar backscatter," J. Phys. Oceanogr. **22**(5), 1033–1045 (1997).
20. J. P. Veefkind, and G. de Leeuw, "A new aerosol retrieval algorithm applied to ATSR-2 data," J. Aerosol Sci. **28**(Suppl. l), 693–694 (1997).
21. K. D. Moore, K. J. Voss, and H. R. Gordon, "Spectral reflectance of whitecaps: their contribution to water-leaving radiance," J. Geophys. Res. **105**(C3 NO. C3), 6493–6499 (2000).
22. Y. Hu, M. Vaughan, Z. Liu, K. Powell, and S. Rodier, "Retrieving optical depth and lidar ratios for transparent layers above opaque water clouds from CALIPSO lidar measurements," IEEE Geophys. And Rem. Sens. Lett. **4**(4), 523–526 (2007).
23. E. Vermote, D. Tanré, J. L. Deuzé, M. Herman, J. J. Morcrette, and S. Y. Kotchenova, "Second Simulation of a Satellite Signal in the Solar Spectrum - Vector (6SV)", *6S User Guide Version 3, November 2006.*
24. H. Gordon, O. Brown, R. Evans, J. Brown, R. Smith, K. Baker, and D. K. Clark, "D. Clark A semianalytic radiance model of ocean color," J. Geophys. Res. **93**(D9), 10909–10924 (1988).
25. A. Morel, and B. Gentili, "Diffuse reflectance of oceanic waters. III. Implication of bidirectionality for the remote-sensing problem," Appl. Opt. **35**(24), 4850 (1996).
26. P. Zhai, Y. Hu, J. Chowdhary, C. Trepte, P. Lucker, and D. Josset, A vector radiative transfer model for coupled atmosphere and ocean systems with a rough interface, Journal of Quantitative Spectroscopy and Radiative Transfer, In Press, Uncorrected Proof, ISSN 0022–4073, DOI: 10.1016/j.jqsrt.2009.12.005, Available online 21 December 2009.
27. C. D. Mobley, *Light and Water: Radiative Transfer in Natural Waters,* San Diego, Academic, (1994).
28. C. M. R. Platt, "Lidar and radiometric observations of cirrus clouds," J. Atmos. Sci. **30**(6), 1191–1204 (1973).
29. J. D. Klett, "Stable analytical inversion solution for processing lidar returns," Appl. Opt. **20**(2), 211–220 (1981).
30. A. Morel, K. J. Voss, and B. Gentili, "Bidirectional reflectance of oceanic waters: A comparison of modeled and measured upward radiance fields," J. Geophys. Res. **100**(C7), 13,143–13,150 (1995).
31. R. M. Measures, *Laser Remote Sensing* (Wiley, New York, 1984)

1. Introduction

Ocean surface return analysis from spaceborne active remote sensing is a promising subject of study. Ocean surface can be used as a target for calibration going from optics to microwave [1–3] and could also provide critical information about state and evolution of the coupled ocean-atmosphere system.

Ocean surface and subsurface return analysis using a lidar instrument has been the subject of several studies over the last three decades. Among several authors, we can cite Bufton [4] who provided the first lidar equation including specular and subsurface terms and Menzies [5] who used a more complete formalism including whitecap reflectance. We used those studies to analyze CALIPSO [6] specular returns and derive quantitative measurements of wind speed [1] and aerosol optical thickness [2]. There are differences in the treatment of specular reflectance by those authors but the usefulness of ocean surface for lidar application has been clearly demonstrated.

Subsurface contribution is a part of the lidar oceanic return [4,5]. The relative importance of this term is expected to increase with larger off-nadir angles and smaller wavelengths. It is negligible for red and infrared wavelengths [4,7] but significant for ultraviolet (UV) [4,5]. We could not observe subsurface influence in our previous work [2] using CALIPSO lidar observations and microwave radiometry. This made us suspect the subsurface contribution at visible wavelengths is lower than what is expected from the commonly accepted formalism [4,5].

With several space-based lidar missions being developed using UV lidars such as the Earth Cloud and Aerosol Radiation Explorer (Earthcare), the Aerosol Cloud Ecosystem (ACE mission), and one with large off-nadir angles (ADM aeolus), a correct formalism to estimate the surface and subsurface return is critical. This further emphasizes the need for a precise determination of the calibration error arising from the use of the ocean as a reference target and for a better understanding of the oceanic subsurface processes.

#128261 - $15.00 USD Received 10 May 2010; revised 2 Jul 2010; accepted 20 Jul 2010; published 12 Oct 2010

For the above reasons, we revisited the ocean lidar equation, taking into account the specific characteristics of emission and reception for this system. To this purpose, we have relied on what has been developed in the last decades for passive and active measurements.

2. Ocean lidar equation

We define the irradiance reflectance R_{ocean} of the ocean surface as

$$R_{ocean} = \frac{F_r}{\mu F_0}. \tag{1}$$

In Eq. (1), F_0 (W.m^{-2}) is the incident irradiance perpendicular to the incident beam and F_r (W.m^{-2}) the radiant emittance of the ocean at surface level. $\mu = \cos(\theta)$, where θ is the incident angle of light with respect to zenith. It will be the off-nadir angle when we will consider a monostatic lidar system. All terms with their units are reported in the Table B.1, B.2, B.3 and B.4 of Appendix B.

The oceanic irradiance reflectance R_{ocean} used in literature [5,8] is written as:

$$R_{ocean} = W \cdot R_{f,eff} + (1-W) \cdot R_S + (1-W \cdot R_{f,eff}) \cdot R_u, \tag{2}$$

where the first term is the contribution from foam patches, expressed as the product of the fraction of the surface covered with whitecaps, *W*, and the effective reflectance of the whitecaps $R_{f,eff}$ (subscript *f* for foam, *eff* for effective); the second term is the specular reflectance R_s (subscript *S* for specular) of the surface waves that are not covered by foam; and the third term describes the contribution from the volume backscattering R_u (subscript *u* for underwater) from the water molecules, suspended material in the water, and for light that penetrates into the water. Those 3 terms, $R_{f,eff}$, R_s and R_u are irradiance reflectance contributions from whitecaps and rough surface at surface level and underwater irradiance reflectance just below the surface level. This formalism was originally used for an analysis of whitecap reflectance using passive measurements (photography) [8]. There are no specular reflections on the area covered by whitecaps which explains the *(1-W)* term. All light not reflected by whitecaps is assumed to be transmitted underwater, explaining the $(1\text{-}W.R_{f,eff})$ term.

$F_{f,eff}$ (W.m^{-2}) and F_S (W.m^{-2}) are the radiant emittance at surface level of the foam patches and ocean rough surface, respectively. R_u is by definition [9] the ratio of the radiant emittance of the ocean just below the surface level F_u^- (W.m^{-2}) to the incident flux per unit area perpendicular to the incident beam F_0^- (W.m^{-2}). The superscript '-' is used to refer to quantities defined just below the ocean surface. As $(1\text{-}W.R_{f,eff})$ is the downward irradiance transmittance of foam patches at surface level ($T_{foam}^{\downarrow}$), Eq. (2) can be rewritten as

$$R_{ocean} = W \cdot \frac{F_{f,eff}}{\mu F_0} + (1-W) \cdot \frac{F_S}{\mu F_0} + T_{foam}^{\downarrow} \cdot \frac{F_u^-}{\mu F_0^-}. \tag{3}$$

The quantities used by Eq. (2) are irradiance. Equation (2) was stated to be equally valid for radiance but in that case "angle dependant reflection function must be introduced" [8] instead of irradiance reflectance which lead to a strong modification of this equation. We found that Eq. (2) does not estimate the subsurface term correctly. Specifically, R_u is the irradiance reflectance for a detector just below the ocean surface. Equation (2) has overlooked the transmission coefficients of the ocean rough surface. This is clearly seen in Eq. (3) where only a one-way transmission coefficient due to foam is present. The downward transmittance due to diffraction by ocean rough surface and the upward transmittance terms are missing.

For a lidar system, Eq. (2) should also be rewritten in terms of the bidirectional reflectance distribution function (BRDF) which is a function of the angles of incidence and reflection.

#128261 - $15.00 USD Received 10 May 2010; revised 2 Jul 2010; accepted 20 Jul 2010; published 12 Oct 2010

The link between the lidar equation and bidirectional reflectance has been derived by Kavaya [10]. We have derived a similar expression in appendix A to allow the reader to better understand the link between the lidar equation and radiative transfer quantities. For this work, it is assumed that the lidar system is pulsed, timegated and that the receiver field of view is larger in extent than the laser footprint on the ocean surface.

We define the lidar surface integrated attenuated backscatter (SIAB) coefficient γ (sr^{-1}) as:

$$\gamma = \int_{R_{\min}}^{R_{\max}} \frac{P_r R^2}{C_L} dR = \frac{E_r}{E_0 \Omega_t}. \tag{4}$$

In Eq. (4), P_r (W) is the optical power collected by the lidar receiver system (telescope); C_L ($W.m^3.sr$) is the lidar system parameter commonly referred to as the lidar constant; R (m) is the range between the lidar transceiver system and the scattering target (molecule, particle, surface). R_{min} and R_{max} define the integration range interval. The range of integration depends on the lidar system and has to be large enough to include all power coming from the surface return, but short enough to avoid or minimize contamination by atmospheric signal. This becomes especially important at large off-nadir angles when the contribution from the surface return is low. In the case of CALIOP, the energy is integrated over several range bins along the line of sight due to the transient response of the system [2]. γ is the ratio of the energy collected by the telescope (E_r in J) per unit of telescope solid angle (Ω_t in sr) on the laser energy emission (E_0 in J). It is the quantity [4] was referring to as the surface reflectance per unit of solid angle (ρ/Ω in his notations), the difference being that we include the atmospheric attenuation inside it.

The BRDF is defined by Eq. (5) as in [11–13]

$$\rho_{BRDF} = \frac{\pi L_r}{\mu F_0}, \tag{5}$$

where ρ_{BRDF} (sr^{-1}) is the BRDF of a reflecting surface. L_r ($W.m^{-2}.sr^{-1}$) is the radiance coming from the surface. Note that there is a difference by a factor π between the BRDF definition of [10] and our work.

Following [10] or Appendix A, we can write:

$$\gamma = \frac{\rho_{BRDF}}{\pi} \mu T_{ATM}^2 = \frac{L_r}{\mu F_0} \mu T_{ATM}^2. \tag{6}$$

$T_{ATM} = exp(-\tau_{ATM}/\mu)$ is the one-way transmittance of the atmosphere for the laser light and τ_{ATM} is the vertical atmospheric optical depth. This equation is valid for the ocean and land when the surface signal is well localized. It is well suited to the specular and foam reflectance at the air-sea interface. It can also be used to analyze subsurface signals, as a common assumption is to treat subsurface return as a reflector just below the surface. In that case, as we will see, the attenuation by ocean surface can also be taken into account as for clouds [14].

For the study of ocean surface layers, the ocean surface integrated attenuated backscatter coefficient γ (sr^{-1}) for a lidar can then be expressed as:

$$\gamma = \gamma_S + \gamma_f + \gamma_u. \tag{7}$$

γ_S, γ_f, and γ_u (sr^{-1}) are the specular, whitecap and subsurface contributions to the SIAB, respectively. Following the definition of BRDF, Eq. (7) can be written as

$$\gamma = \left(W \cdot \frac{L_{f.eff}}{\mu F_0} + (1-W) \cdot \frac{L_S}{\mu F_0} + T_{ocean}^{\downarrow} t_{ocean}^{\uparrow} \cdot \frac{L_u^-}{\mu F_0^-} \right) \mu T_{ATM}^2. \tag{8}$$

#128261 - $15.00 USD Received 10 May 2010; revised 2 Jul 2010; accepted 20 Jul 2010; published 12 Oct 2010

In Eq. (8), $L_{f,eff}$ (W.m^{-2}.sr^{-1}) and L_S (W.m^{-2}.sr^{-1}) are the upward radiances at surface level by foam patches and ocean rough surface, respectively. L_u^- (W.m^{-2}.sr^{-1}) is the upward radiance of the ocean just below the surface level. $T_{ocean}^{\downarrow}$ is the oceanic downward irradiance transmittance at surface level. As upward quantities are radiance and not irradiance, the upward transmittance at surface level should be expressed in terms of radiance instead of irradiance and is therefore noted as $t_{ocean}^{\uparrow}$.

Ignoring the contribution of foam [4], used the scattering cross section expression of [15] and suggested the use of the following expression for the SIAB.

$$\gamma = T_{ATM}^2 \left(\frac{\rho}{4\pi < S^2 > \cos^4(\theta)} \exp\left(\frac{-\tan^2(\theta)}{< S^2 >} \right) + \frac{R_u}{\pi} \cos(\theta) \right), \quad (9)$$

where ρ (sr^{-1}) is the Fresnel reflectance coefficient [4] at nadir angle and $<S^2>$ is the variance of the wave slope distribution more commonly referred to as the mean square slope (MSS) [5,15].

The ocean wave slope variance $<S^2>$ assuming a Gaussian distribution can be expressed as a first approximation by the Cox & Munk [16] model:

$$\left\langle S^2 \right\rangle = 0.003 + 0.005v. \quad (10)$$

In Eq. (10), v is the wind speed in m/s measured at 12 meters above the ocean surface.

Using the work of [5] leads to the derivation of another expression of SIAB (Eq. (14) of [17]).

$$\gamma = T_{ATM}^2 \left(\frac{(1-W)\rho}{2\pi < S^2 > \cos^4(\theta)} \exp\left(\frac{-\tan^2(\theta)}{< S^2 >} \right) + W.\frac{R_{f,eff}}{\pi} \cos(\theta) + \left(1 - W \cdot R_{f,eff}\right) \frac{R_u}{\pi} \cos(\theta) \right). \quad (11)$$

Menzies used [4] but argued a 2π factor should be used instead of the 4π, stating "Because Barrick derived a backscatter cross section per unit surface area, it should be normalized by 2π rather than by the 4π used by Bufton *et al"*.

Our results show that only the term expressing the reflectance of whitecaps in Eq. (11) may be appropriate. We will develop our own derivation for each term of Eq. (7) in the following subsections.

2.1 Specular reflectance

The contribution of specular return for active remote sensors has been theoretically derived by Barrick [15] in terms of normalized scattering cross section. Bréon and Henriot [18] have derived the specular BRDF for a rough surface (See Eq. (4) in [18]) that can be used along with Eq. (6) for the lidar. Thus, γ_S can be expressed for a θ off-nadir angle:

$$\gamma_S = \frac{(1-W)\rho}{4\cos^5(\theta)} p(\varsigma_x, \varsigma_y) T_{ATM}^2 \approx \frac{(1-W)\rho}{4\pi < S^2 > \cos^5(\theta)} \exp\left(\frac{-\tan^2(\theta)}{< S^2 >} \right) T_{ATM}^2. \quad (12)$$

$p(\varsigma_x, \varsigma_y)$ is the probability of slopes of waves ς_x and ς_y in both along- and cross-wind directions, respectively. Assuming isotropicity and the probability distribution of wave slopes $p(\varsigma_x, \varsigma_y)$ to be gaussian, Eq. (12) reduces to the well known exponential distribution of the only parameter $<S^2>$. One can see the specular lidar return expressions of Eq. (9) and (11) were not correct.

For nadir pointing, the error arising when using a gaussian model of MSS can be estimated using the work of [19]. The deviation from gaussianity can be estimated by *n/(n-1)* where *n* is the peakedness coefficient. For optical sensors, the deviation has been found to be between 2% and 14%, when the wind speed varies from 3 m/s to 15 m/s. The highest uncertainty value is equivalent to the use of the Gram-Charlier coefficients of [16] or [18]. Following the results

#128261 - $15.00 USD Received 10 May 2010; revised 2 Jul 2010; accepted 20 Jul 2010; published 12 Oct 2010

of [18], using a gaussian model would lead to an overestimation of the specular return from 13% to 11% between 1 and 10 m/s. This 2% variation can be considered a bias within actual lidar calibration and wind speed retrieval accuracies. Error arising from assuming gaussianity is not expected to go higher than 14%, but future research should be performed to assess it more accurately.

2.2 Whitecaps reflectance

Whitecaps are assumed to behave like a lambertian surface [8,20]. The increase of lidar return at high wind speed present in CALIPSO observations [2] is consistent with treating the whitecaps as a lambertian surface and the fraction of the surface covered with whitecaps, *W,* as a power law of wind speed. The power law we found [2] is within the range of what can be found in literature [7]. So far, lidar observations seems to be in agreement with the formalism used by [5]. As for a lambertian surface $F_{f,eff} = \pi L_{f,eff}$, the derivation of the lidar signal coming from whitecaps leads to the following equation [5]:

$$\gamma_f = W.\frac{R_{f,eff}}{\pi}\cos(\theta)T_{ATM}^2. \tag{13}$$

There are not a lot of studies about whitecap influence on lidar returns and more work on the subject is recommended. To increase lidar equation accuracy, a better characterization of the term shown by Eq. (13) will be needed in the future, especially at high wind speeds when bubbles are forming inside the water column [21]. The exact physical process of bubble formation has yet to be fully understood, but the lidar depolarization information could be used to get new insights into this phenomena. It has been applied with success for liquid water spherical droplets [22] and could be used for spherical bubbles using a similar approach. In that case, the foam would contribute to the subsurface return, but further study is needed to better understand this effect.

2.3 Subsurface reflectance

The subsurface return is treated by some radiative transfer codes [23] and has also been well studied by other authors in terms of water leaving radiance [24,25]. Those previous works contain most of what is needed to update Eq. (2). In the following subsection, we will simply adapt them in the frame of the lidar equation formalism.

2.3.1 Air/sea interface transmittance

The subsurface term used in the previous formalism [5,8] represents a lambertian surface situated just below the surface [9]. The main flaw of this formalism is that it does not account for the directional downward and upward transmittance correctly.

The downward transmittance by the foam free surface has been overlooked in Eq. (2). This is especially important at low wind speeds when whitecap influence is negligible. The downward transmittance $T_{ocean}^{\downarrow}$ for irradiance is:

$$T_{ocean}^{\downarrow} = 1 - W \cdot R_{f,eff} - (1-W)R_s(\theta). \tag{14}$$

In Eq. (14), R_s is the specular irradiance reflectance for a rough ocean surface. To evaluate R_s, one needs to integrate the exact bidirectional reflection matrix for a rough ocean surface (see Eq. (29) in Zhai et al. [26]). Figure 1 shows the specular reflectance as a function of incident angle for three wind speeds, 3, 7, and 11 m/s. The ocean water refractive index is assumed to be 1.338. The influence of linear polarization is shown, R_{par} is the irradiance reflectance when the incident light polarization is parallel to the scattering plane, R_{perp} refer to the same quantity when the polarization is perpendicular to the scattering plane. Therefore, R_S values range between R_{par} and R_{perp}, depending on the incident light polarization. One can note that the specular irradiance reflectance is dependent on the incident angle value.

#128261 - $15.00 USD Received 10 May 2010; revised 2 Jul 2010; accepted 20 Jul 2010; published 12 Oct 2010

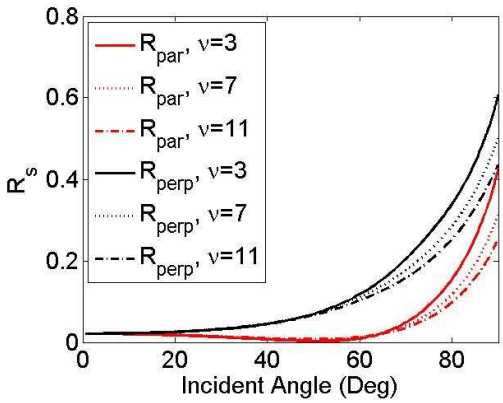

Fig. 1. Specular reflectance as a function of incident angle for three wind speeds, 3, 7, and 11 m/s.

It is obvious that the specular reflectance is mostly flat for incident angles smaller than 20 degrees. A rough estimation of the specular reflectance is:

$$R_s \approx 0.0209 \cdot (1 \pm 0.05). \tag{15}$$

Equation (15) is valid for angles of incidence smaller than 10 degrees and wind speeds less than 11 m/s. The uncertainty of 5% is due to variations in the polarization of the laser beam, the angle of incidence, and the wind speed. Specifically, if one needs to know a number beyond the accuracy of 5%, the angle between the plane of the linear polarization of the laser and the incident meridian plane needs to be known. While the Cox & Munk model provides a simplified approach, it allows an easy calculation. Using the recent derivation of $<S^2>$ for a space-based lidar [1,2] would only change the relationship between wind speed and wave slope variance, whereas light scattering is a function of the surface roughness state. The resultant effect would be a slight change in the applicable wind speed range.

The upward transmittance term is not mentioned in Eq. (2), whereas it is obvious that the light reflected by the subsurface water body has to cross the ocean-air interface to reach the detector. It is a direct consequence of the definition of the subsurface reflectance R_u [9] and cannot be ignored. To accurately calculate this term, one needs to know the slope surface distribution as well as the exact upwelling radiance distribution, which is normally unknown in the lidar applications. Future lidar missions will offer more information about the subsurface term and determine if some simple assumptions can be used. To take the ocean transmittance into account, the following equation used for upward radiance $t_{ocean}^{\uparrow}$ is:

$$t_{ocean}^{\uparrow} = (1-W)t_s + W.t_{foam}. \tag{16}$$

In Eq. (16), t_s is the ocean interface transmittance for radiance propagating to the zenith on the area not covered by whitecaps, and t_{foam} is the upward transmittance due to whitecaps for radiance. Multiple scattering will be introduced later.

It is known that t_s is only slightly dependant on wind speed [24]. Here we use the flat surface as an approximation. Hence:

$$t_s = \frac{T_s(\theta')}{m^2}. \tag{17}$$

In Eq. (17), T_s is the irradiance transmittance for the ocean-air interface on the area not covered by whitecaps. As we are using flat surface as an approximation, it is equal to the Fresnel irradiance transmittance which slowly changes with incident angle variations.

#128261 - $15.00 USD Received 10 May 2010; revised 2 Jul 2010; accepted 20 Jul 2010; published 12 Oct 2010

$T_s \approx 0.979$ for normal incidence angles, θ' is the underwater incident angle (θ being the angle of refraction, following Snell's law). T_s variations are less than 1% for θ' between 0 and 30% but reaches 0 beyond the critical angle (48.4 degrees). $m \approx 1.338$ is the refractive index for ocean water. The m^2 term is a consequence of the so called n-squared law [27]. There is a fundamental difference between transmission coefficients of irradiance and radiance which has to be taken into account within the lidar equation.

Assuming whitecaps behaves as a lambertian surface, t_{foam} can be easily expressed as a function of the irradiance reflectance for foam patches $R_{f,eff}$.

$$t_{foam} = \frac{1 - R_{f,eff}}{\pi}. \tag{18}$$

An assumption is made in Eq. (18) that whitecaps possess the same reflectance for upward and downward incident light. We are not aware of any underwater measurements of the irradiance reflectance of whitecaps which would confirm or disprove this assumption. We also neglected the formation of bubbles at high wind speed which could change the underwater irradiance reflectance in an unknown way. All those effects would need a better quantification, far beyond the scope of this theoretical work.

2.3.2 Subsurface reflectance value

The subsurface reflectance [9] R_u is used by all previous authors [4,5] using the lidar subsurface equation. Using the correct treatment of ocean upward and downward transmittance (Eq. (14) and Eq. (16) allows us to revisit this formalism for the lidar equation. As will be discussed in Section 3.0, this will lead to the value of subsurface SIAB in better agreement with our previous work. We believe it is important to understand the link between the subsurface reflectance [9] R_u and the lidar equation used for atmospheric targets. This will be discussed in the following part. The subsurface contribution of the lidar return should be written:

$$\gamma_u = T_{ocean}^{\downarrow} t_{ocean}^{\uparrow} T_{ATM}^2 \int_{S_{\min}}^{S_{\max}} \beta_u \exp(-2\int_{s_{\min}}^{s_{\max}} \eta_u \alpha_u ds) dS. \tag{19}$$

In Eq. (19), S is the optical path (one should note that, for a lidar system, as the speed of light is lower in water than in air, the vertical resolution Δz is reduced underwater), β_u is the underwater backscatter coefficient ($m^{-1}.sr^{-1}$), α_u (m^{-1}) is the underwater extinction coefficient, and η_u is the multiple scattering coefficient [28]. This coefficient contains only the in-water multiple scattering and not the air-sea interface/subsurface multiple scattering whose influence is small (around 0.5% in Eq. (21) and has been neglected here. This could however be included in this coefficient with a simple change of definition. Assuming β_u and α_u are constant within the considered optical path and considering the high attenuation of water, the integrated term would be equal to [29]

$$\int_{S_{\min}}^{S_{\max}} \beta_u \exp(-2\int_{s_{\min}}^{s_{\max}} \eta_u \alpha_u ds) dS = \frac{\beta_u}{2\eta_u \alpha_u}. \tag{20}$$

Even if the two expressions are different, the backscatter coefficient in the numerator and extinction (due to absorption and scattering) in the denominator shows strong analogies with the expression derived by Morel $\frac{f'}{Q}\frac{b_b}{a+b_b} = \frac{R_u}{Q}$ [25]. b_b is the underwater backscattering coefficient (hemispherical integration of the phase function in the backward direction), a is the underwater absorption coefficient. Q (sr) expresses the ratio of underwater radiant emittance F_u^- ($W.m^{-2}$) to underwater radiance L_u^- ($W.m^{-2}.sr^{-1}$) and defines angular variation of underwater radiance distributions. f' is an empirical coefficient linking the irradiance

#128261 - $15.00 USD Received 10 May 2010; revised 2 Jul 2010; accepted 20 Jul 2010; published 12 Oct 2010

reflectance to the water's inherent optical properties b_b and a. For lidar applications, it expresses the link between the integrated quantities b_b and with the backscatter quantities β_u and α_u as well as the increase of extinction when multiple scattering coefficient is present with respect to single scattering extinction. Both Q and f' are dependent on direction and water properties. As f' and Q contain the directionality information, the formalism used by Eq. (2) using R_u instead of Eq. (20) can be used for the lidar equation, at least for a first order approximation. To improve the accuracy, the exact similitude between integrated quantities and what is measured by the lidar will be the subject of future research.

3. Discussion

At first order, the lidar equation for an off-nadir angle θ can be expressed as

$$\gamma = T_{ATM}^2 \left(\begin{array}{l} \dfrac{(1-W)\rho}{4\pi < S^2 > \cos^5(\theta)} \exp\left(\dfrac{-\tan^2(\theta)}{< S^2 >} \right) \\ +W.\dfrac{R_{f,eff}}{\pi}\cos(\theta) \\ +\dfrac{\left(1-W\cdot R_{f,eff}-(1-W)R_s(\theta)\right)\left[(1-W)\right]}{\left(1-\bar{r}R_u\right)}\cos(\theta)\dfrac{T_s(\theta')}{m^2}\dfrac{R_u}{Q(\theta')} \\ +\dfrac{\left(1-W\cdot R_{f,eff}-(1-W)R_s(\theta)\right)}{\left(1-R_{f,eff}R_u\right)}W\left(\dfrac{1-R_{f,eff}}{\pi}\right)\cos(\theta)R_u \end{array} \right). \quad (21)$$

$\bar{r}$ is the water–air Fresnel irradiance reflectance for the whole diffuse upwelling irradiance, and is of the order of 0.48 [18]. The multiple scattering term $\left(1-\bar{r}R_u\right)$ takes into account the downward, internal reflection at the interface [25]. The same formalism $\left(1-R_{f,eff}R_u\right)$ is used for multiple scattering at the ocean-air interface where foam patches are present.

To better understand the advancement that this new equation represents, it is useful to make the comparison with Eq. (9) and Eq. (11). One can see all terms are different except the whitecaps reflectance.

Our expression of the subsurface term has never been used like this in the lidar field. Its exact value is dependant on wind speed and off-nadir angle. However we can discuss the magnitude of the modification expected with respect to the previous formalism. As it is the case for most ocean studies using lidar, and as there is still some work to be performed on the subsurface effect of whitecaps, W will be assumed equal to 0. In that case, the subsurface term of Eq. (21) has to be compared with R_u/π at nadir. The exact value of Q depends on the lidar incident angle, but a range between π and 5 is a reasonable estimation [24,25] for off-nadir angle up to 30 degrees [30]. Assuming $R_u = 0.01$ [4] at 532 nm, the subsurface coefficient of Eq. (21) is between 0.53 R_u/π and 0.34 R_u/π. This lower value is consistent with our analysis of CALIPSO ocean surface echo [2] in which the subsurface contribution is not significant.

Previous studies using large off nadir angles [5,17] did not find values of subsurface return lower than that given by Eq. (2). However, as those studies were using a 2π factor instead of 4π in the specular reflectance term, this lowers the relative difference between the subsurface and specular term and the global factor 2 bias can come from the uncertainty of the lidar calibration, and the wind speed estimation or surface roughness model as the Cox and Munk model [16] is an approximation [1].

Here we find that the differences range from 89% (0.53 R_u/π) to 194% (0.34 R_u/π).

It is recommended that, for future lidar applications, Eq. (21) should be used. Additional research will need to be conducted to further improve the accuracy. Specifically, improvements to Eq. (21) would include the probability of slope distribution in the cross and

#128261 - $15.00 USD Received 10 May 2010; revised 2 Jul 2010; accepted 20 Jul 2010; published 12 Oct 2010

upwind components [18], as well as to gain a better understanding of the subsurface term given by Eq. (20). There is also a need to better assess the large uncertainties associated with the lidar return of foam patches and their effect on subsurface lidar returns.

4. Conclusion

We revisited the formalism to be used for the analysis of the lidar ocean surface and subsurface returns (Eq. (21). The previous formalism had weaknesses in specular return angular dependency and would lead to an overestimation of the subsurface contribution by a factor of two to three. This improved lidar equation is more consistent with the latest advances in radiative transfer theory. This advancement will have a direct impact on the scientific outcome of future space-based lidar missions, and will more accurately determine some of the coefficients critical to ocean color research and their directional dependencies.

Appendix A

The power received by the telescope can be expressed as in the classical lidar equation formalism (see Eq. (7).23 of [31] for elastic scattering when the wavelength of observation is the same as that of the laser)

$$P_r(R) = \frac{C_L}{R^2}\beta(R)T_{ATM}^2(R). \tag{A.1}$$

In Eq. (A.1), P_r is the optical power (in W) collected by the lidar receiver system (telescope). C_L is the lidar system parameter commonly referred as the lidar constant (in $W.m^3.sr$). R is the range (in m) between the lidar transceiver system and the scattering target (molecule, particle, surface). β is the backscatter coefficient ($m^{-1}.sr^{-1}$). $T_{ATM} = exp(-\tau_{ATM}/\mu)$ is the one-way transmittance of the atmosphere for the laser light and τ_{ATM} is the vertical atmospheric optical depth. As we will discuss the surface return, which is at a specific and well determined range, the dependence of the different variables with R will not been shown in the following equations.

By definition, the lidar constant C_L is

$$C_L = \frac{c}{2}E_0A_t. \tag{A.2}$$

In Eq. (A.2), A_t is the telescope area (m^2), c the speed of light ($m.s^{-1}$) and E_0 the laser energy emission (J). Here a perfect efficiency of the receiver is assumed. It is also assumed a perfect transceiver alignment and all emitted light is collected by the telescope (i.e. the telescope field of view is larger than the laser beam divergence and the diffraction occurs far enough from the lidar system so there is no overlap problem).

When studying the surface, it is necessary to write the lidar equation in a different way. The power received by the telescope coming from the surface is equal to

$$P_r = L_r A_t \Omega_G \exp\left(-\frac{\tau_{ATM}}{\mu}\right). \tag{A.3}$$

L_r is the upward radiance ($W.m^{-2}.sr^{-1}$) at the surface level and Ω_G is the solid angle (sr) from which the surface is seen from the telescope (subscript G for ground).

This solid angle is by definition:

$$\Omega_G = \frac{A_G\mu}{R^2}. \tag{A.4}$$

A_G is the area of the laser footprint. It is the real area on the ground, so it is a function of μ but using the real area is the standard way to define the solid angle of the surface.

The BRDF of the surface is by definition [11–13]

#128261 - $15.00 USD Received 10 May 2010; revised 2 Jul 2010; accepted 20 Jul 2010; published 12 Oct 2010

$$\rho_{BRDF} = \frac{\pi L_r}{\mu F_0}. \quad (A.5)$$

F_0 (W.m^{-2}) is the incident flux per unit area perpendicular to the incident beam.

Combining (A.4) and (A.5) with (A.3) we get

$$P_r = \frac{\mu F_0 \rho_{BRDF}}{\pi} A_t \frac{A_G \mu}{R^2} \exp\left(-\frac{\tau_{ATM}}{\mu}\right). \quad (A.6)$$

F_0 can also be written as the laser emitting power P_0 per unit area projected perpendicular to the incident beam and attenuated by the atmospheric absorption and scattering

$$F_0 = \frac{P_0}{\mu A_G} \exp\left(-\frac{\tau_{ATM}}{\mu}\right). \quad (A.7)$$

Introducing (A.7) inside (A.6), we get:

$$P_r = \frac{\mu \rho_{BRDF}}{\pi} \frac{P_0}{\mu A_G} \exp\left(-\frac{\tau_{ATM}}{\mu}\right) A_t \frac{A_G \mu}{R^2} \exp\left(-\frac{\tau_{ATM}}{\mu}\right). \quad (A.8)$$

As $\int P_0 dt = E_0$, we can rewrite (A.8) using the lidar constant (A.2)

$$\int P_r dt = \frac{\rho_{BRDF}}{\pi} \frac{1}{A_G} \frac{A_G \mu}{R^2} \exp\left(-2\frac{\tau_{ATM}}{\mu}\right) C_L \frac{2}{c}. \quad (A.9)$$

As the surface level is well defined there is no time dependency on the right side of Eq. (A.9) and using $dt = 2dR/c$ we can express the BRDF as a function of lidar surface integrated attenuated backscatter (SIAB) coefficient γ (sr^{-1}) as in Eq. (A.10)

$$\int \frac{P_r R^2}{C_L} \frac{c}{2} dt = \gamma = \frac{\rho_{BRDF}}{\pi} \mu \exp\left(-2\frac{\tau_{ATM}}{\mu}\right). \quad (A.10)$$

Coming back to its definition, the SIAB is (for a scatterer at a given altitude) the ratio of the energy collected by the telescope ($\int P_r dt = E_r$) per unit of telescope solid angle ($\Omega_t = A_t/R^2$) on the laser energy emission E_0 as written in Eq. (A.11).

$$\gamma = \frac{E_r}{E_0 \Omega_t}. \quad (A.11)$$

Appendix B: Index

Table B.1. Index of different terms used in this manuscript

Index of the different terms used in this study				
Variable	**Link with other variables**	**Definition**	**Unit**	**Notes**
θ		Incident angle of light with respect to the zenith	rad.	For this study, θ mainly refers to the lidar off-nadir angle
μ	cos (θ)	Cosine of incident angle of light	No unit	
θ'		Under water incident angle of light with respect to the zenith	rad.	Conterpart of θ following Snell's law

#128261 - $15.00 USD Received 10 May 2010; revised 2 Jul 2010; accepted 20 Jul 2010; published 12 Oct 2010

Table B.2. Index of different terms used in this manuscript (continued)

Index of the different terms used in this study				
Variable	**Link with other variables**	**Definition**	**Unit**	**Notes**
R_{ocean}	$\frac{F_r}{\mu F_0}$	Irradiance reflectance of the ocean surface	No unit	
$R_{f,\,eff}$	$\frac{F_{f,eff}}{\mu F_0}$	Irradiance reflectance of foam patches	No unit	
R_S	$\frac{F_S}{\mu F_0}$	Irradiance reflectance of ocean rough surface (specular return)	No unit	
R_u	$\frac{F_u^-}{\mu F_0^-}$	Irradiance reflectance of ocean just below the surface level (underwater)	No unit	
F_r		Radiant emittance of the ocean at surface level	$W.m^{-2}$	
$F_{f,eff}$		radiant emittance of foam patches	$W.m^{-2}$	
F_S		radiant emittance of ocean rough surface	$W.m^{-2}$	
F_u^-		radiant emittance of the ocean just below the surface level	$W.m^{-2}$	
F_0		Incident flux per unit area perpendicular to the incident beam at surface level	$W.m^{-2}$	It is the (atmospheric attenuated) solar constant for passive measurements
F_0^-		incident flux per unit area perpendicular to the incident beam just below the surface level	$W.m^{-2}$	
W		Fraction of the surface covered with whitecaps	No unit	
$T_{foam}^{\downarrow}$	1-W.$R_{f,eff}$	downward irradiance transmittance of foam patches at surface level	No unit	
$T_{ocean}^{\downarrow}$		Oceanic downward irradiance transmittance at surface level	No unit	

Table B.3. Index of different terms used in this manuscript (continued)

Index of the different terms used in this study				
Variable	**Link with other variables**	**Definition**	**Unit**	**Notes**
$t_{ocean}^{\uparrow}$		Oceanic upward radiance transmittance at surface level	No unit	
T_S		Ocean (without foam) interface transmittance for irradiance propagating to the zenith	No unit	Assumption of flat ocean is made in this study
t_S	$\frac{T_s}{m^2}$,	Ocean (without foam) interface transmittance for radiance propagating to the zenith	No unit	Assumption of flat ocean is made in this study
t_{foam}		upward transmittance of foam patches for radiance at surface level	No unit	
m		refractive index for ocean water	No unit	
γ	$\frac{E_r}{E_0\Omega_t}$	surface integrated attenuated backscatter (SIAB) coefficient	sr^{-1}	Ratio of the energy collected by the telescope per unit of telescope solid angle on the laser energy emission.

#128261 - $15.00 USD Received 10 May 2010; revised 2 Jul 2010; accepted 20 Jul 2010; published 12 Oct 2010

γ_S		contributions of the specular return to the surface integrated backscatter coefficient	sr^{-1}	
γ_f		contributions of the foam patches to the surface integrated backscatter coefficient	sr^{-1}	
γ_u		contributions of the subsurface to the surface integrated backscatter coefficient	sr^{-1}	
ρ_{BRDF}	$\frac{\pi L_r}{\mu F_0}$	Bidirectionnal reflectance distribution function (BRDF)	sr^{-1}	BRDF is a function of the angle of incidence and reflection
L_r		radiance of the surface	$W.m^{-2}.sr^{-1}$	
$L_{f,eff}$		radiance of the surface by foam patches	$W.m^{-2}.sr^{-1}$	
L_S		radiance of the surface due to specular return	$W.m^{-2}.sr^{-1}$	
L_u^-		radiance of of the ocean just below the surface level	$W.m^{-2}.sr^{-1}$	
ρ		Fresnel reflectance coefficient at nadir angle	sr^{-1}	
$<S^2>$		variance of the wave slope distribution	No unit	Also called mean square slope (MSS)
$p(\varsigma_x, \varsigma_y)$		probability of slopes of waves	No unit	ς_x and ς_y are the slopes along- and cross-wind directions.

Table B.4. Index of different terms used in this manuscript (continued)

Index of the different terms used in this study

Variable	Link with other variables	Definition	Unit	Notes
v		wind speed	$m.s^{-1}$	measured at 12 meters above the ocean surface
β_u		underwater backscatter coefficient	$m^{-1}.sr^{-1}$	
α_u		underwater extinction coefficient	m^{-1}	
η_u		Underwater multiple scattering coefficient	No unit	
Q	$\frac{F_u^-}{L_u^-}$	ratio of underwater radiant emittance to underwater radiance	sr	
f'		empirical coefficient	No unit	It links the irradiance reflectance to the water inherent optical properties b_b and a
b_b		underwater backscattering coefficient	m^{-1}	hemispherical integration of the phase function in the backward direction
a		underwater absorption coefficient	m^{-1}	
$\bar{r}$		water–air Fresnel reflection for the whole diffuse upwelling irradiance	No unit	
P_d		optical power collected by the lidar receiver (telescope)	W	
C_L		lidar system parameter	$W.m^3.sr$	commonly referred as the lidar constant
R		range between the lidar transceiver system and the scattering target (molecule, particle, surface)	m	c is the speed of light t is the time
E_r	$\int P_r dt$	energy collected by the telescope, coming from the surface	J	P_r (W) is the power collected by the lidar receiver system, coming from the surface

#128261 - $15.00 USD Received 10 May 2010; revised 2 Jul 2010; accepted 20 Jul 2010; published 12 Oct 2010

Ω_t		Telescope solid angle seen from the surface	sr	
E_0	$\int P_0 dt$	Laser energy emission (laser impulse)	J	P_0 (W) is the power emitted by the lidar system (laser impulse power)
T_{ATM}	$exp(-\tau_{ATM}/\mu)$	one-way transmittance of the atmosphere	No unit	
τ_{ATM}		Atmospheric vertical optical depth	No unit	
S		Optical path	m	

Acknowledgments

This work has been supported by NASA Postdoctoral Program (NPP) at NASA Langley Research Center administered by Oak Ridge Associated Universities. Science Systems and Applications Inc. (SSAI) is greatly acknowledged for their support. We would like to thank the two anonymous reviewers for suggesting corrections and improvements to the manuscript.

#128261 - $15.00 USD Received 10 May 2010; revised 2 Jul 2010; accepted 20 Jul 2010; published 12 Oct 2010